Solid-State Electronics Vol. 28, No. 7, pp. 677–687, 1985
Printed in Great Britain.

0038-1101/85 $3.00 + .00

A TIME- AND TEMPERATURE-DEPENDENT TWO-DIMENSIONAL SIMULATION OF GTO TURNOFF PROCESS II—INDUCTIVE LOAD CASE

AKIO NAKAGAWA
Toshiba Research and Development Center, 1 Komukai Toshiba-cho, Saiwai-ku, Kawasaki, 210, Japan

(*Received* 22 *February* 1984; *in revised form* 11 *June* 1984)

Abstract—Two-dimensional simulation was carried out for the GTO thyristor turnoff process under an inductive load with 34 A (3400 A/cm^2) initial anode current and 7.2 A gate current, which is the same condition as that in which a significant current concentration into a small part of a device area was experimentally observed. A 24,000 A/cm^2 maximum anode current density is reached during the turnoff process in the reduced "on-region" (see text for the definition). The on-region width in the p-base reduces rapidly to 70 μm and remains at around 60 μm until the device is completely turned off. It is shown that a large amount of the stored n-base carriers in the current concentrated area are removed by the developing high electric field region in the n-base. This results in a large dV/dt current, which sustains the high current density in the current concentrated area.

1. INTRODUCTION

Recent advances in Gate-Turn-Off Thyristor (GTO) development have enabled 4500 V, 2400 A devices to appear on the market[1]. Theoretical research on the device turn-off mechanism has progressed along with the device development using computer simulation technologies[2–4]. In 1975, thyristor current voltage characteristics were numerically simulated for the first time[5]. Since then, a number of papers[3, 5, 6, 7] have been published on thyristor characteristics simulation. There were a few papers published dealing with the GTO turnoff failure mechanism [2–4]. All of them stressed the importance of the anode voltage role in the turnoff process. Anode voltage increase rate, as well as the value itself, are both factors strongly influencing the turnoff failure process. According to [3], there is a maximum anode voltage limit V_A(MAX) which can be applied to the device while a part of the device is still conducting a high current density in the turnoff process (when current concentration into a small part of the device area is occurring).

$$V_A(\mathrm{MAX}) = E_h \cdot W_{NB}, \tag{1}$$

where E_h is the magnitude of the high electric field appearing in the n-base ($1 \sim 2 \times 10^4$ V/cm), and W_{NB} is the n-base width (cm). The same paper predicted, by using a one-dimensional GTO turnoff model, that a large amount of stored n-base carriers in the current concentrated area are removed by the high electric field region developing in the n-base of the current concentrated area. The excess carrier removal from the n-base was supported by an experiment[2] using an infrared observation technique. In the present paper, a two-dimensional model is introduced to simulate the phenomena for the case of a high anode current density and a high turn-off gain. A new insight in regard to the turn-off process is also surveyed under inductive load conditions.

2. MATHEMATICAL MODEL

The model utilized in the present calculation includes heavy Doping Effects (H.D.E.)[8], Fermi statistics[9], Auger recombination[10], carrier to carrier scattering[10] etc. The effects of Fermi statistics are included by introducing parameter W_n for electrons[9, 11].

$$N_c \exp\frac{1}{kT}(qW_n + F_n - E_c) \equiv \int_{E_c}^{\infty} \frac{\rho(E)\,dE}{1 + \exp\dfrac{E - F_n}{kT}}, \tag{2}$$

where N_c is the effective density of states, E_c is the conduction band edge energy, ρ the density of states function and F_n the Fermi energy. The current equation under a nonisothermal case is derived from Boltzmann transport equation by adopting the relaxation time approximation[12].

$$J_n = -\frac{q}{m^2}\int d^3p\,\tau_e \frac{\partial f^\circ}{\partial E} p_x^2 \left[\frac{\partial F_n}{\partial x} + \frac{E - F_n}{T}\frac{\partial T}{\partial x}\right], \tag{3}$$

where m is the effective mass, f the distribution function, τ_e the relaxation time. Substituting (2) into (3), the following current equation is obtained in a procedure similar to that in[13].

$$J_n = \mu_n kT\frac{\partial n}{\partial x} - q\mu_n n\frac{\partial \psi}{\partial x} + q\mu_n n\frac{\partial}{\partial x}\left(\frac{\Delta E_c}{q} - W_n\right) - \mu_n kTn\frac{\partial}{\partial x}(\ln N_c) + \mu_{2n} kn\frac{\partial T}{\partial x} + q\mu_n n\frac{W_n}{T}\frac{\partial T}{\partial x}, \tag{4}$$

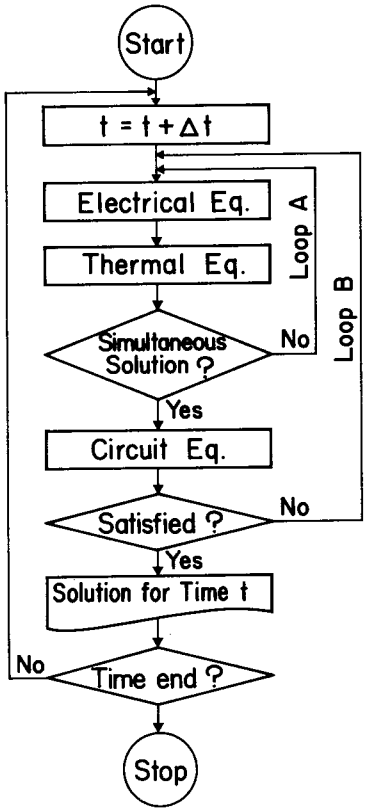

Fig. 1. Flow-chart for solution process.

where

$$\mu_{2n} = -\frac{q}{m^2 kTn}\int d^3p\,\tau_e p_x^2 (E - E_c)\frac{\partial f^\circ}{\partial E}, \quad (5)$$

$$E_c = E_{c0} + \Delta E_c, \quad (6)$$

$$\frac{\partial E_{c0}}{\partial x} = -q\frac{\partial \psi}{\partial x} \quad (7)$$

and E_{c0} is the conduction band edge energy for nondoped silicon. It should be emphasized that the deviation in diffusion coefficient D from $\mu kT/q$ is taken into account in the term $-q\mu_n \partial W_n/\partial x$. The corresponding hole current equation can be obtained in a similar way.

Equation (4) is simplified by the following assumptions:

$$N_c = 2\left(\frac{2\pi mkT}{h^2}\right)^{3/2} (m = \text{const}), \quad (8)$$

$$\mu_{2n} = 2\mu_n \text{ [13]}. \quad (9)$$

The last term in (4) can be ignored, if a temperature increase occurs in a high resistivity area, where W_n is almost zero.

The basic equations for the four variables: electron, hole, electric potential and temperature, were solved by the Newton and SLOR combination method [11]. The basic solution process is shown in a flowchart (Fig. 1). The heat flow equation was separately treated. Loop A was executed to obtain simultaneous solutions for the four variables. The SLOR method was found to be effective for the present calculation. The optimum SLOR iteration number was 10 ~ 20 for each Newton cycle.

3. CALCULATED RESULTS

Calculations were carried out for the same device structure (200 μm × 5 mm emitter area) as in the previous paper [11]. A 9 × 55 rectangular mesh was used to discretize the four basic equations. The minority carrier lifetime in the n-base was assumed to be 1 μsec. All the other carrier lifetimes for each grid point were determined by the formula used in paper [9], depending on the local impurity density. Electron lifetime was assumed to be four times as large as hole lifetime.

A calculation was carried out for the case where 34 A (3400 A/cm^2) anode current was turned off with an 8 μH inductive load and 7.2 A gate current. This condition is the same as that in which a significant current concentration in a small part of the device area was experimentally observed. A voltage clamp circuit was attached instead of the usual snubber circuit to prevent the device from being subjected to more than 200 V anode voltage. The impurity doping

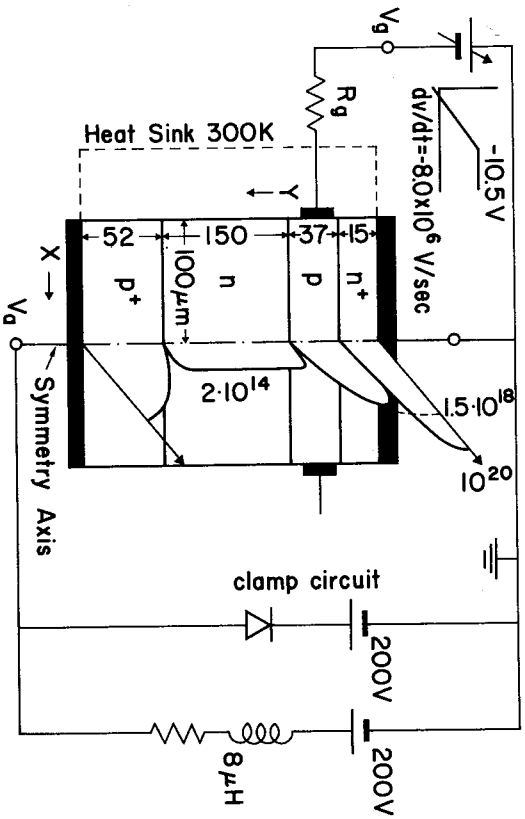

Fig. 2. Schematic diagram for the analyzed system.

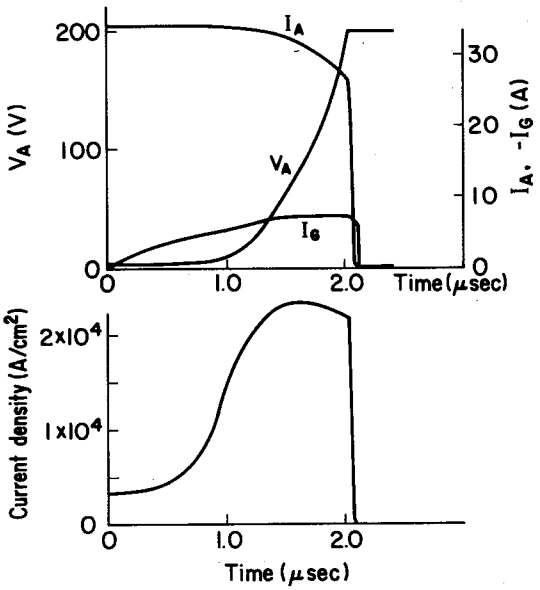

Fig. 3. Calculated turnoff waveform (upper trances) and current density change at the center of the middle junction (lower trace).

profile and the circuit configurations are given in Fig. 2. Temperature at the ohmic contact is fixed at 300 K as well as at the imaginary surface (indicated by the dashed line in Fig. 2), which is assumed to be 60 μm remote from the side wall where the gate contact is placed.

Figure 3 shows calculated waveforms for anode voltage, current and gate current. Storage-time is 1.7 μsec and the fall-time is as short as 0.4 μsec, owing to the anode voltage clamp circuit. Upon application of negative gate bias, p-base carrier plasma is squeezed, resulting in a decrease in the current conducting area in the p-base as well as an increase in the current density in the conducting area. The lower trace in Fig. 3 shows the current density change with time lapse at the center of the middle junction. It reaches a peak value of 24,000 A/cm^2 at 1.54 μsec and continues to stay around this high value until the voltage clamp circuit begins to work. The peak current density is usually reached at the end of the storage time or in the early period of the fall-time, depending upon the environmental circuit conditions[7]. The current density at the center of the middle junction rapidly decreases after the anode voltage is clamped at 200 V. The same results were reached, as reported in papers[3,4], wherein using the voltage clamp circuit is an effective way to help

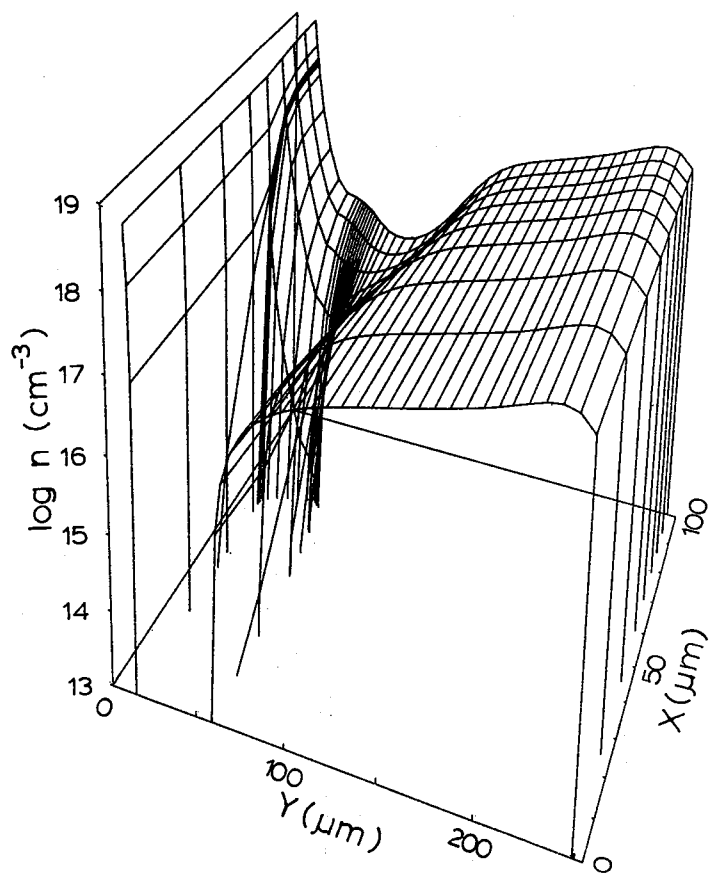

Fig. 4. Electron density distribution for $t = 1.32$ μsec.

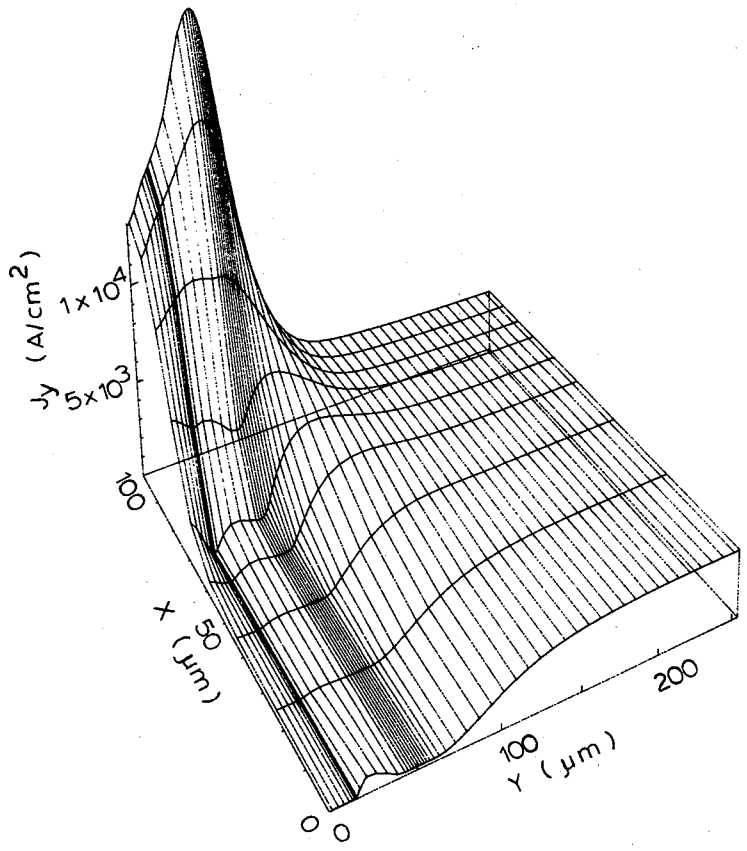

Fig. 5. Y-component of the current density distribution for $t = 1.32$ μsec.

the device turn off. In other words, the anode voltage increase rate is a direct cause to induce current concentration.

According to reference[11], "off-region" is tentatively defined especially for electrons as the area where electron density is less than 10^{14} cm^{-3}. Then the "on-region" is the rest of the device area, except for the two emitter layers. These concepts are defined only for the two bases and the three junction layers. The meaning of the off-region is the area where almost all of the injected excess carriers are removed. The meaning of the on-region is the reverse. Electron current density in the off-region should be almost zero from the definition.

Upon application of the negative gate bias, excess carriers in a part of the p-base, which is near the gate electrode, and in the adjacent parts of gate-cathode and middle junctions, are removed from the gate electrode, resulting in a decrease in the on-region width for the p-base. Extraction of the excess carriers initially proceeds in a way similar to the resistive load case[11]. Figure 4 shows the electron density distribution for the 1.32 μsec time step. By this time, the on-region width in the p-base has been reduced to 66 μm, within which most of the anode current is flowing. Figure 5 shows the Y-component of the current density distribution corresponding to Fig. 4. The 22,000 A/cm^2 high current density is seen at the center of the middle junction. On the contrary, the current still flows almost uniformly in the n-base because of the highly modulated conductivity.

Figure 6 shows the electric potential distribution at the 1.43 μsec time step. Even in the reduced on-region in the p-base and the middle junction, the electric field is relatively high and conducts extremely high electric current density, whereas the electric field in the middle junction of the off-region (depletion layer) is high and is sustained by the fixed space charges.

Figure 7 shows the electron density distribution at the 2.02 μsec time step: just before the anode voltage reaches 200 V. The high electric field region has extended far into the n-base, as shown in Fig. 8, having swept out a large amount of the carriers in the n-base. The removed n-base carriers make a large dV/dt current, which works as positive gate current and sustains anode current flow. Figure 9 shows the same phenomena from a different angle. The dotted region in the figure shows the high electric field region of more than 1×10^4 V/cm. Equal carrier density lines are shown in the figure for the 10^{14}, 10^{15}, 10^{16} and 10^{17} cm^{-3} electron density levels. A thick line, denoted by 10^{14} cm^{-3} electron density, also shows the boundary between on- and off-regions. The on-region changes its width rapidly

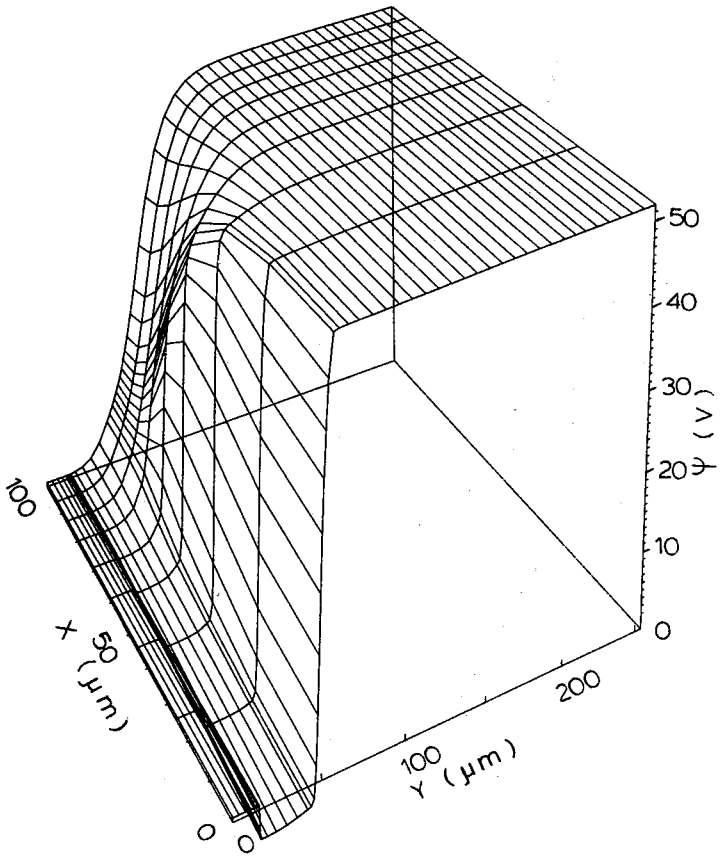

Fig. 6. Electric potential distribution for $t = 1.43$ μsec.

within the high electric field region. It is easily seen that the high electric field is expanding into the n-base, mostly in the on-region.

It was shown in the one-dimensional model calculations [3] that the electric field magnitude in the high electric field region is approximately determined by the local ratio of electron current density over hole current density (J_n/J_p). However, in the two-dimensional cases, the electric field magnitude is determined in a more complex way, because a part of the hole current flows into the off-region across the on- and off-region boundary. However, the current ratio (J_n/J_p) is still a dominant factor to determine the high electric field magnitude in the on-region.

Turnoff gain G and npn transistor current gain α_{npn} are expressed by the following equations.

$$G = (I_n + I_p)/I_G, \tag{10}$$

$$\alpha_{npn} = I_n/(I_n + I_p - I_G), \tag{11}$$

where I values are the total hole or electron currents which flow across an equal potential line, which crosses the high electric field region. These values remain almost the same within the high electric field region, because carrier recombination is small there.

The ratio I_n/I_p is given as

$$I_n/I_p = \frac{\alpha_{npn}(G-1)}{G(1-\alpha_{npn}) + \alpha_{npn}}. \tag{12}$$

If I_n/I_p is assumed to be almost the same as the local ratio J_n/J_p, then the following equation holds, because almost all of the current flows by drift in the high electric field region, where electron and hole densities are almost equal to each other (high injection condition):

$$\frac{\mu_n(E_h)}{\mu_p(E_h)} \cong \frac{\alpha_{npn}(G-1)}{G(1-\alpha_{npn}) + \alpha_{npn}}. \tag{13}$$

The high electric field magnitude E_h is uniquely determined from the above equation if $E_h > 1 \times 10^4$ V/cm, because μ_n/μ_p value strongly depends on electric field E_h, as shown in Fig. 10. As stated already, a part of the hole current flows from the on-region into the off-region and becomes gate current. Then, the ratio J_n/J_p gradually changes within the high electric field region. Figure 11 shows the Y components of hole and electron current densities at the middle junction. Fifteen percent of the hole current flows in the off-region at the 2.02 μsec time

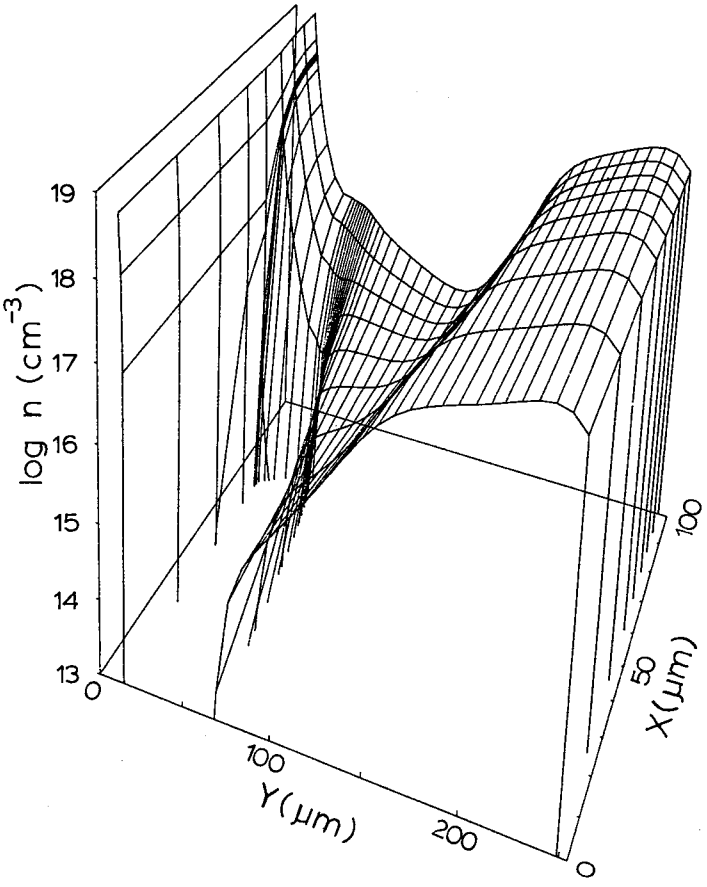

Fig. 7. Electron density distribution for $t = 2.02$ μsec.

step. If r% of the total hole current flows within the on-region, eqn (13) should be replaced by

$$\frac{\mu_n(E_n)}{\mu_p(E_h)} \cong \frac{100}{r} \cdot \frac{\alpha_{npn}(G-1)}{G(1-\alpha_{npn})+\alpha_{npn}}. \quad (14)$$

r is a function of position Y and becomes larger from the middle junction toward the anode-side-end of the high electric field region. Thus, electric field magnitude E_h increases from the middle junction toward the anode side for a while, although current density decreases.

If turnoff gain is small, E_h, determined by eqn (14), becomes large. It follows that the high electric field region appearing in the on-region is thin, and that the amount of carriers removed from the n-base becomes small, resulting in a small dV/dt current with anode voltage recovering. This situation makes the device easy to turn off, because the dV/dt current is assumed to sustain current in the current concentrated area[3]. It should be noted that the initial tail current value becomes large in return for this case, because a large amount of carriers are left in the n-base.

Continuing the analysis for the 2.02 μsec time step, the high electric field development in the n-base slightly changes the current flow pattern, from that shown in Fig. 5 to that shown in Fig. 12.

Once the anode voltage is clamped at 200 V, the turnoff process is markedly accelerated. This is because the high electric field region does not expand toward the p-emitter in the n-base any more. Figure 13 will be used to interpret the turnoff phenomena for the final on-region. In the figure, the electron density distributions along the symmetry axis ($X =$ 100 μm line) are shown with time step as a parameter. The arrows indicate the directions of the principal changes in the distributions. The decrease in the carrier density corresponds to the electric field buildup there. Until the anode voltage reaches 200 V, carriers adjacent to the high electric field region are removed by the high field region expansion, while the carrier density within the high field region remains almost unchanged, because the current density does not decrease due to the inductive load nature. In other words, the removed n-base carriers make a large dV/dt current, which sustains anode current flow. After the clamp circuit begins to work, the change in the electron density distribution varies its pattern. The carrier density within the high electric field region begins to decrease rapidly and the electric field magnitude increases, resulting in device

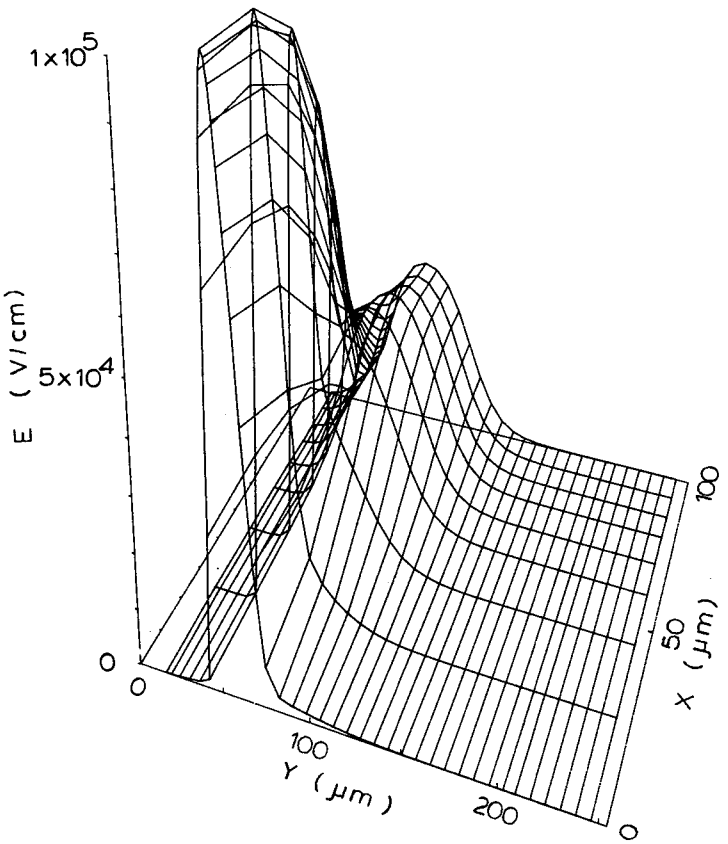

Fig. 8. Electric field distribution for $t = 2.02$ μsec.

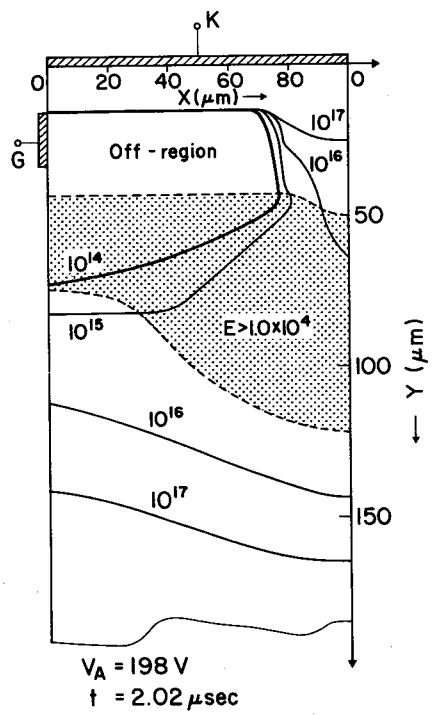

Fig. 9. Equal carrier density lines, high electric field region and off-region.

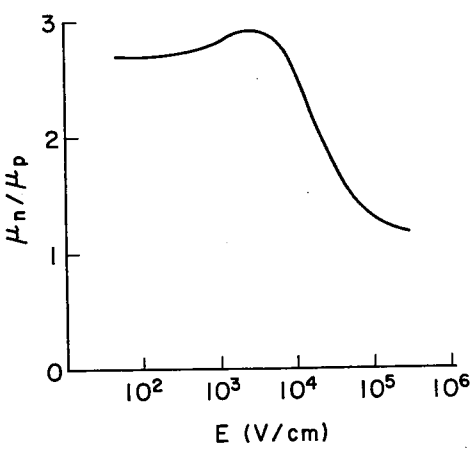

Fig. 10. Electric field dependence of the mobility ratio μ_n/μ_p.

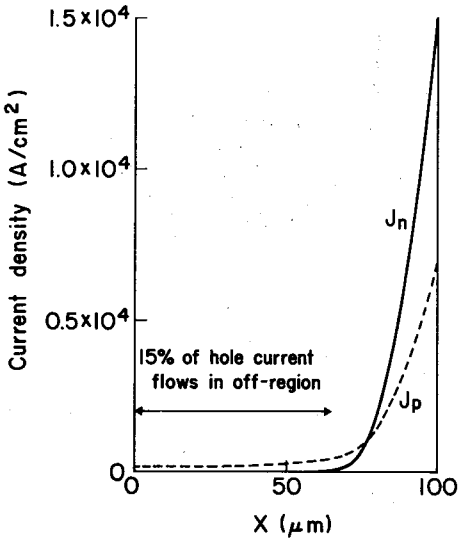

Fig. 11. *Y*-components of hole and electron current densities at the middle junction.

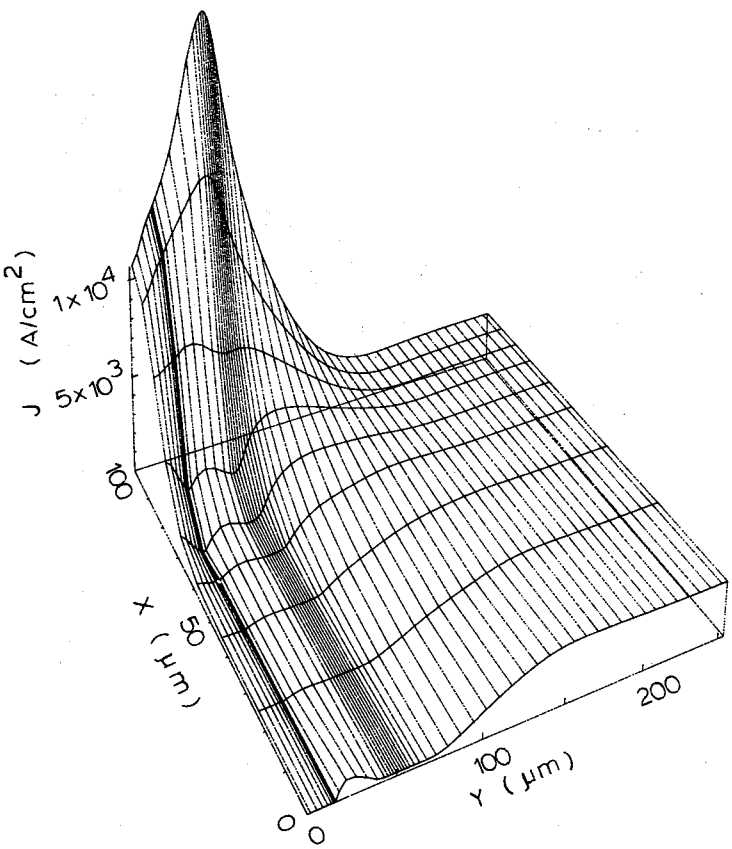

Fig. 12. *Y*-component of the current density distribution for $t = 2.02$ μsec.

resistance increase as well as a rapid decrease in anode current. The high electric field region thickness shrinks until the real depletion layer appears. It should be emphasized that the carrier density gradient from *p*-emitter to the depletion layer (the middle junction) is relatively small after the device turn-off, because a part of the stored *n*-base carriers has already been removed. This results in the tail current being significantly small, as seen in Fig. 3. However, this fact cannot always be seen in experiments, be-

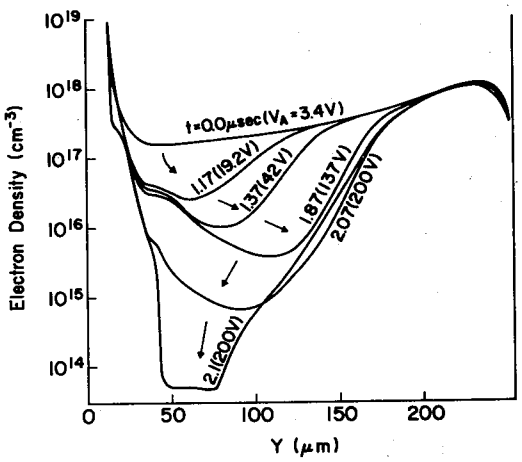

Fig. 13. Electron density distributions for the device center along $X = 100$ μm line.

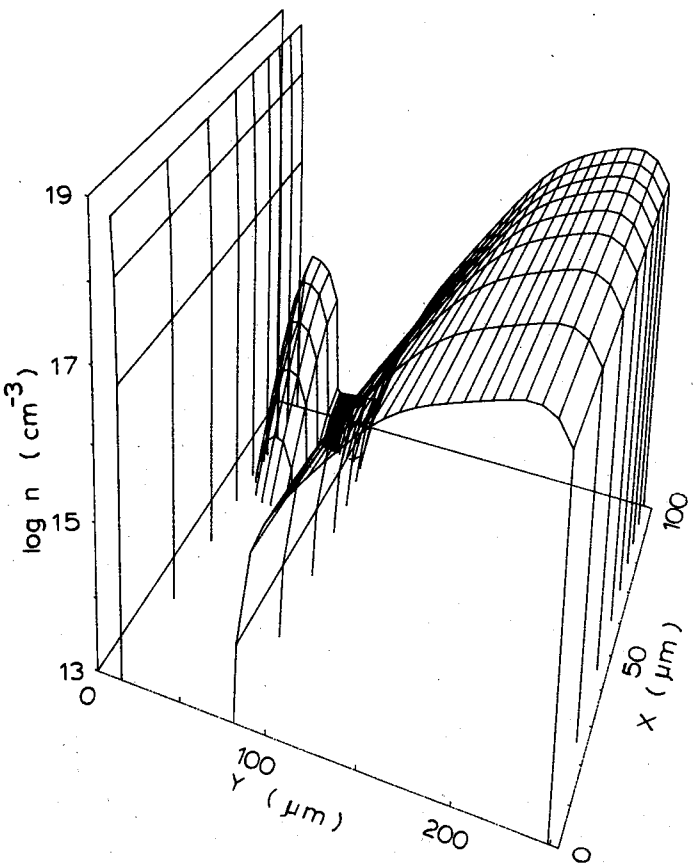

Fig. 14. Electron density distribution for $t = 2.17$ μsec.

cause, for most devices, the final on-region is only a small portion of the total device area and the tail current is still large in the early turned-off portions of a device, where a large amount of n-base excess carriers still remains.

Figure 14 shows the electron density distribution for the 2.17 μsec time step just after anode current is completely turned-off. While the stored carriers in the n-emitter–p-base junction of the final on-region are being removed with all of the middle junction being recovered, the gate current becomes larger than the anode current for a moment.

Figure 15 shows the temperature distribution at the 2.11 μsec time step. The peak temperature of

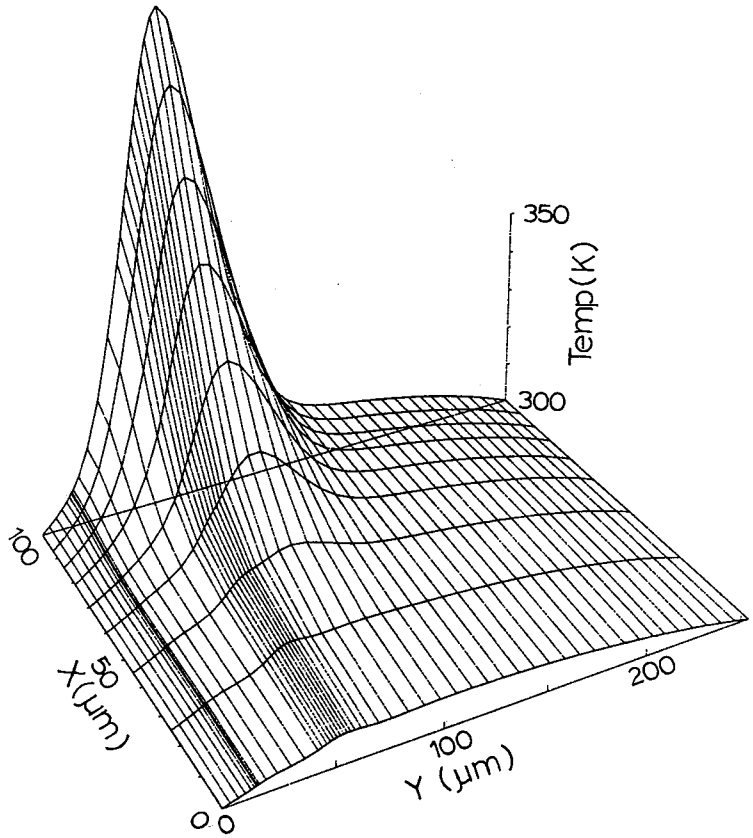

Fig. 15. Temperature distribution for $t = 2.11$ μsec.

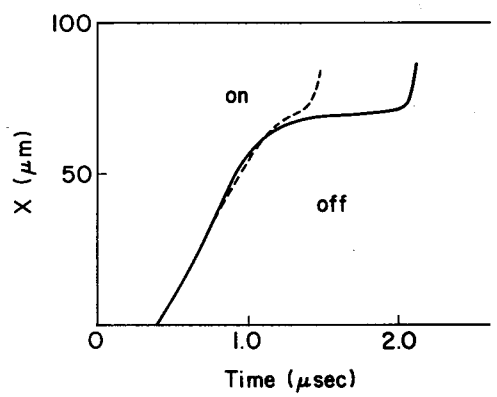

Fig. 16. Change in boundary location with time lapse on the $Y = 19$ μm line (broken line denotes the pure resistive load case[7, 11].

420 K is seen just inside the n-base near the middle junction. The 120 degree local temperature increase is relatively small for causing significant changes in the turnoff process, except for the local mobility reduction, which results in a device resistance increase.

4. DISCUSSIONS

Figure 16 shows the time-variation in the boundary between on- and off-regions on the $Y = 19$ μm line in the p-base. The boundary actually means the location where the carrier density is 10^{14} cm^{-3}. The on-region width reduces rapidly to a value of 70 μm (the half width is shown in the figure) and stays around 60 μm until the whole device is turned off. After the on-region width reaches around 60 μm, the whole system behaves like a one-dimensional system and the excess carrier removal from the n-base is accelerated. Thus, as far as the present calculations (including the calculations in paper[11]) are concerned, the maximum turnoff gain should be determined, not by the two-dimensional theory[14] but by the following one-dimensional theory.

$$G_{\max} = \frac{\alpha_{npn}}{\alpha_{npn} + \alpha_{pnp} - 1} \tag{15}$$

The present results for an inductive load case should be compared with those for a resistive load case[11]. In the inductive load case with a voltage clamp circuit (which is a practical case), the turnoff process is characterized by three phases. In the first phase (storage-time), neither anode voltage or current change. In the second phase, anode current is almost constant while anode voltage recovers. In the third phase, anode current decreases. Each phase approximately corresponds to the following change inside the device. In the first phase, p-base excess

carriers are squeezed to the final limit. In the second phase, the n-base excess carriers are removed by the high electric field region developing in the n-base. The carrier density within the high electric field region is kept almost constant. In the third phase, the carrier density inside the high electric field region is rapidly reduced.

In the resistive load case, the second and third phases cannot be distinguished, because both anode voltage and current have to change at the same time. Turnoff gain G decreases as anode current decreases, since gate current does not decrease until anode current becomes almost zero. Thus, when anode voltage recovers, the magnitude of the appearing high electric field, determined from eqn (14), is higher than in the inductive load case, because G is smaller. It follows that the high electric field region is thinner and does not expand farther into the n-base than the inductive load case.

Calculated results were compared with the experimental results[2] obtained by infrared observation technique. The observed final on-region width was 80 μm, which is close to the calculated result, 60 μm. The carrier density decrease was also observed widely in the n-base[2] when high anode current was turned off. This is assumed to be direct evidence for the excess carrier removal from the n-base, which occurs when both high anode voltage and high current density appear at the same time with a high turnoff gain.

The grid number in the x-direction is greater than the previous calculation by 2[7,11]. However, the final on-region width in the p-base is exactly the same as before. Moreover, the curve in Fig. 16 coincides with the previous results (the dotted line in Fig. 16 shows a resistive load case[11]) except for the latter part of the trace-curve. Thus, the author considers that the 7 or 9 grid points in the x-direction are probably sufficient for the present calculation.

5. CONCLUSION

A two-dimensional GTO turnoff process has been simulated under an inductive load, including heat dissipation for a case of 34 A anode current and 7.2 A gate current, which is the same condition as that in which a significant current concentration was experimentally observed. Upon negative gate bias application, the on-region width reduces rapidly to 70 μm and then stays around 60 μm until the whole device is turned off. After the on-region width reaches 60 μm, the whole system behaves like a one-dimensional system. Excess carriers in the n-base of the final on-region are removed by the developing high electric field in the n-base with anode voltage recovering. This makes a large dV/dt current and is assumed to sustain the high current density in the current concentrated area. The highest current density more than 2×10^4 A/cm^2 is observed in the reduced final on-region. The amount of carriers removed from the n-base in the turnoff process depends on turnoff gain G as well as npn three layer current gain α_{npn} in the high injection level.

REFERENCES

1. T. Shinohe, K. Takigami and M. Azuma, International Power Electronics Conference Record (IPEC-Tokyo), p. 75, (1983).
2. H. Ohashi and A. Nakagawa, *IEEE 1981 IEDM Technical Digest*, p. 414.
3. A. Nakagawa and H. Ohashi, *IEEE Trans. Electron Devices*, **ED-31**, 273 (1984).
4. T. Nagano, H. Fukui, T. Yatsuo and M. Okamura, PESC 1982 Record, p. 383.
5. W. Anheier, W. L. Engl, O. Mank and A. Wieder, *IEEE 1975 IEDM Technical Digest*, p. 363.
6. M. Kurata, *Solid-St. Electron.*, **19**, 527 (1976).
7. A. Nakagawa and D. H. Navon, *IEEE 1982 IEDM Technical Digest*, p. 496.
8. R. J. van Overstraeten, H. DeMan and R. Mertens, *IEEE Trans. Electron Devices*, **ED-20**, 290 (1973).
9. A. Nakagawa, *Solid-St. Electron.*, **22**, 943 (1979).
10. M. S. Adler, *IEEE Trans. Electron Devices*, **ED-25**, 16 (1978).
11. A. Nakagawa and D. H. Navon, *IEEE Trans. Electron Devices*, **ED-31**, 1156 (1984).
12. A. H. Marshak and K. M. van Fliet, *Solid-St. Electron.*, **21**, 417 (1978).
13. R. Stratton, *IEEE Trans. Electron Devices*, **ED-19**, 1288 (1972)
14. E. D. Wolley, *IEEE Trans. Electron Devices*, **ED-13**, 590 (1966).